Journal of Optoelectronics and Advanced Materials Vol. 7, No. 6, December 2005, p. 3093 - 3100

MATHEMATICAL STUDY OF METAL NANOPARTICLE SIZE DETERMINATION BY SINGLE X-RAY LINE PROFILE ANALYSIS

N. Aldea[*a], B. Barz[♣b], T. D. Silipas[a], F. Aldea[c], Z. Wu[d]

[a]National Institute of R&D of Isotopic and Molecular Technologies, P.O. Box. 700, RO 400293 Cluj-Napoca, Romania
[b]University of Missouri - Columbia, 223 Physics Building, MO 65211, USA
[c]Agriculture and Medicine Veterinary University, Department of Mathematics and Computer Science, RO 400372 Cluj-Napoca, Romania
[d]Coordination Laboratory of National Center for Nanoscience and Nanotechnology, Synchrotron Radiation Facilities of Beijing Electron Positron Collider, People's Republic of China

The new theoretical outline for determination of the metal crystallite nanosize and lattice strain from X-ray diffraction line profile broadening is discussed. Emphasis is made on the rigorous analysis of the line profiles in terms of Fourier transform. Fermi generalized distribution function for single X-ray line profile approximation is used in order to determine the crystallite size and the lattice strain by the deconvolution technique. The microstructural parameters are obtained by the use of the Warren and Averbach theory and are included in the general form of the Fourier transform of the true sample. A comparison of microstructural models of the supported nickel catalysts determined by various analytical approximations is presented. Practical examples that emphasize the influence of the ideal standard line profiles of supported nickel catalysts as experimental samples are given. The measurements were performed on Beijing Synchrotron Radiation Facilities.

(Received October 3, 2005; accepted November 24, 2005)

Keywords: Deconvolution, Fourier transform, X -ray diffraction, Metal crystallite size, Microstrain

1. Introduction

X-ray diffraction line profile analysis is a versatile nondestructive method that can be used in obtaining nanostructural information (averaged over a moderately large volume about 1 mm^3) about supported metal catalysts used in oxidation, redaction, isotopic exchange and hydrogenation reactions. From the position and broadening of X-ray line profile (XRLP) are obtained the imperfect crystallite structure in terms of effective crystallite size and microstrain as lattice disorder.

The purpose of this paper is to point out theoretical aspects of determining the metal nanoparticle size and the lattice distortion using various analytical approximations as well as general formula based on Warren and Averbach theory. The results are exemplified by analyzing two samples of nickel catalysts: 85 at. % Ni/Cr_2O_3 and 98.8 at. % Ni/UO_2. The analytical models are implemented in our XRSIZE computer package program.

[*] Corresponding author: naldea@s3.itim-cj.ro
[♣] On leave from National Institute of R&D of Isotopic and Molecular Technologies, RO 400293 Cluj-Napoca, Romania

2. Theoretical background - procedures for X-ray line profile analysis

X-ray diffraction pattern of a crystal can be described in terms of scattering intensity as function of scattering direction defined by the scattering angle 2θ, or by the scattering parameter s=2sin θ/λ, where λ is wavelength of the incident radiation. Experimentally one can measure the integrated intensity profile function *h(2θ)* or *h(s)* for the crystals. We shall discuss the X-ray diffraction for the mosaic structure model in which the atoms are arranged in blocks, each block itself being an ideal crystal, but with adjacent blocks not accurately fitted together. The experimental X-ray line profile (XRLP), *h*, represents the convolution between the true sample *f* and the instrumental function produced by a well-annealed sample, g, and it is described by the Fredholm integral equation of the first kind [1]:

$$h(s) = \int g(s - s^*) f(s^*)\, ds^* \tag{1}$$

From mathematical point of view, the true sample function, *f(s)*, as a solution of eq. (1) can be obtained by three distinct methods: Fourier transform [2], regularization [3, 4] and the third order spline functions [5]. If one chooses the first one, the true sample function can be obtained by the relationship,

$$H(L) = G(L)F(L), \tag{2}$$

where *F(L)*, *H(L)* and *G(L)* are Fourier transforms (FT) of the true sample, experimental XRLP and instrumental function, respectively. The variable *L* is the distance perpendicular to the *(hkl)* reflection planes. The crystallite size and lattice disorder can be analyzed as a set of the independent events of likelihood concept. The normalized *F(L)* can be described as the product of two factors, $F^{(s)}(L)$ and $F^{(\varepsilon)}(L)$. The factor $F^{(s)}(L)$ describes the contribution of crystallite size and stocking fault probability while the factor $F^{(\varepsilon)}(L)$ gives information about the microstrain of the lattice. Based on Warren and Averbach theory [6], the general form of the Fourier transform of the true sample for cubic lattices is given by relationships,

$$F^{(s)}(L) = e^{-\frac{|L|}{D_{eff}(hkl)}}, F^{(\varepsilon)}(L) = e^{-\frac{2\pi^2 \left\langle \varepsilon_L^2 \right\rangle_{hkl} h_0^2 L^2}{a^2}}, \tag{3}$$

where $D_{eff}(hkl)$ is the effective crystallite size, $\langle \varepsilon^2 \rangle_{hkl}$ is the microstrain of the lattice, $h_0^2 = h^2 + k^2 + l^2$ and $C^2 = 2\pi^2 h_0^2 / a^2$.

It is known that whenever two or more X-ray line profiles (XRLP) of the same (*hkl*) plane family are present, the particle size and the lattice disorder effects can be separated. Raitieri, Senin and Fagherazzi [7] investigated the global structure of Cu filings for (111) and (222) XRLP and their results are based on following relation,

$$\ln F(L) = \ln F^s(L) - 2\pi^2 \left\langle \varepsilon_L^2 \right\rangle_{hkl} L^2 \frac{h_0^2}{a^2} \tag{4}$$

Their structural results are obtained by linear analyzing of eq. (4) as shown in Fig. 1. X-ray line broadening investigations of the nanostructured materials such as supported metal catalysts have been limited to find the average crystallite size from the integral breadth or the full width at half maximum (FWHM) of a diffraction profile. In the case of supported metal catalysts, it is impossible to obtain two orders of the same *(hkl)* profile due to the difficulty of performing satisfactory intensity measurements on the higher-order reflections. Consequently, it is not possible to apply the classical method of Warren [1].

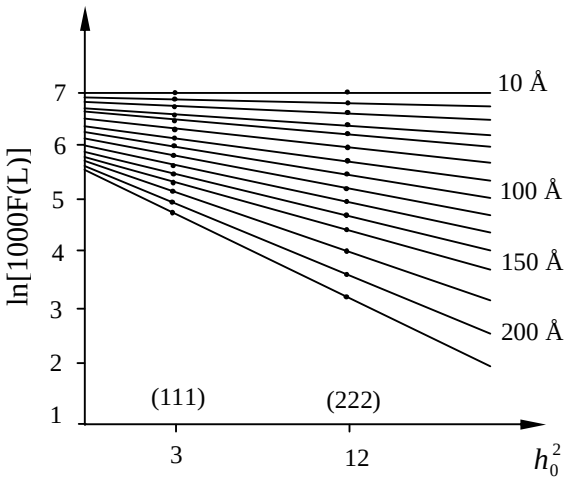

Fig. 1. Ln[1000 F(L)] as a function of $h_0^2 = h^2 + k^2 + l^2$ for several L values, (111)-(222) orders of XRLP. Cu sample cold-worked at room temperature.

Despite the numerous studies, the global microstructure parameters based on single XRLP analysis are incompletely elaborated because many authors have used the approximate relations for Fourier transform of the true sample. Some of them are given in Table 1.

The integral width $\delta^{[F]}$ of the Fourier transform of the true sample from eq. (3) contains the crystallite size as well as the microstrain of the lattice and it is given by relationship,

$$\delta^{[F]}(\beta,\gamma) = \sqrt{\frac{\pi}{\beta}} \exp\left[\frac{\gamma^2}{4\beta}\right] \cdot \left[1 - erf\left(\frac{\gamma\sqrt{\beta}}{2\beta}\right)\right], \tag{5}$$

where $\beta = \frac{2\pi^2 \langle \varepsilon_L^2 \rangle h_0^2}{a^2}$, $\gamma = \frac{L}{D_{eff}}$ and *erf* is the error function [21]. For large crystallite size $(\gamma \to 0)$ the integral width can be approximated with the relation

$$\delta^{[F]}(\beta,\gamma) = \sqrt{\frac{\pi}{\beta}} - \frac{\gamma}{\beta} \tag{6}$$

If we take into consideration the uncertainty relations between integral widths of direct and inverse Fourier transforms [22, 23], we can estimate $\delta^{[f]}$ by the relation,

$$\delta^{[f]}\delta^{[F]} \geq \frac{1}{4\pi} \tag{7}$$

The general form of the true sample function *f(s)* is given by inverse Fourier transform of *F(L)*

$$f(s) = \int_{-\infty}^{\infty} e^{-\beta L^2 - \gamma|L|} e^{2\pi i s L} dL =$$

$$= \sqrt{\frac{\pi}{\beta}} \exp\left[\frac{\gamma^2 - (2\pi s)^2}{4\beta}\right] \left\{ \mathrm{Re}\left[erfc\left(\frac{\gamma - 2\pi i s}{2\sqrt{\beta}}\right)\right] \cos\frac{\pi\gamma s}{\beta} - \mathrm{Im}\left[erfc\left(\frac{\gamma + 2\pi i s}{2\sqrt{\beta}}\right)\right] \sin\frac{\pi\gamma s}{\beta} \right\}, \tag{8}$$

where $s = 2\left(\frac{\sin\theta}{\lambda} - \frac{\sin\theta_0}{\lambda}\right)$ and *erfc* is the complementary error function [21].

Table 1. Single X ray line profile analysis.

References	Assumptions	Procedures
R. S. Smith [8]	$F^{(s)}(L)=1-\frac{L}{D_{eff}}$, $F^{(\varepsilon)}(L)=\cos(2\pi h_0^2 <\varepsilon^2>_{hkl} L^2/a^2)$	Determination of D_{eff} and $<\varepsilon^2>_{hkl}$ by curve fitting
G. B. Mitra [9]	$F^{(\varepsilon)}(L)=\exp(-2\pi h_0^2 <\varepsilon^2>_{hkl} L^2/a^2)$	$\frac{dF}{dL}=-\frac{1}{D_{eff}}$ for $L\to 0$; $\ln\left[\frac{F(L)}{1-L/D_{eff}}\right]$ $vs.L^2$; slope $(L\to 0)=-2\pi h_0^2 <\varepsilon^2\rangle_{hkl}$
J. Mignot [10]	$F^{(s)}(L)=1-\frac{L}{D_{eff}}$, $F^{(\varepsilon)}(L)=1-2\pi h_0^2\langle\varepsilon^2\rangle_{hkl} L^2/a^2$	Determination of D_{eff} and $<\varepsilon^2>_{hkl}$ by curve fitting
J. Mignot [11]	$F^{(s)}(L)=1-\frac{L}{D_{eff}}$, $F^{(\varepsilon)}(L)=\exp(-2\pi h_0^2\langle\varepsilon^2\rangle_{hkl} L^2/a^2)$	Determination of D_{eff} and $<\varepsilon^2>_{hkl}$ by curve fitting
E. J.Charlson et al. [12] P. Ganesen et al. [13] N. Aldea et al. [14-20]	For small crystallites $(L\to 0)$: (i) $F(L)=1-L/D_{eff}-C^2<\varepsilon^2(L)>_{hkl} L^2 + C^2<\varepsilon^2(L)>_{hkl} L^3/D_{eff}$, (ii) $F(L)=a_0+a_1L+a_2L^2$	(i) Determination of D_{eff} and $<\varepsilon^2>_{hkl}$ by curve fitting; (ii) By assumption $<\varepsilon(L)>_{hkl}=K/L$, $a_0=1$, $a_1=-(1/D_{eff}+C^2K)$, $a_2=C^2K/D_{eff}$

The integral width of the narrow true sample function $(\gamma\to 0)$ can be expressed with the relation

$$f(s)=\sqrt{\frac{\pi}{\beta}}\exp\left[\frac{\gamma^2-(2\pi s)^2}{4\beta}\right]\left\{\begin{array}{l} erfc\left(\frac{\gamma}{2\sqrt{\beta}}\right)-\frac{(\pi)^{\frac{3}{2}}\exp\left[-\frac{\gamma^2}{4\beta}\right]}{\beta^{\frac{3}{2}}}s^2\cos\frac{\pi\gamma s}{\beta}+ \\ \frac{2\sqrt{\pi}\exp\left[-\frac{\gamma^2}{4\beta}\right]}{\sqrt{\beta}}s+\frac{1}{3}\frac{(\pi)^{\frac{5}{2}}(2\beta-\gamma^2)\exp\left[-\frac{\gamma^2}{4\beta}\right]}{\beta^{\frac{5}{2}}}s^3\sin\frac{\pi\gamma s}{\beta} \end{array}\right\} \quad (9)$$

The functions of $F^{(s)}(L)$ and $F^{(\varepsilon)}(L)$ can be described as the Fourier transform of the following two distributions: Cauchy, P_C, and gaussian, P_G

$$e^{-\frac{|L|}{D_{eff}}}=2D_{eff}FT\left[\frac{\left(\frac{1}{D_{eff}}\right)^2}{\left(\frac{1}{D_{eff}}\right)^2+4\pi^2s^{*2}}\right] \quad \text{and} \quad e^{-\frac{2\pi^2\langle\varepsilon_L^2\rangle h_0^2 L^2}{a^2}}=FT\left[\frac{a}{h_0\sqrt{2\pi\langle\varepsilon_L^2\rangle}}-e^{-\frac{a^2s^{*2}}{2\langle\varepsilon_L^2\rangle h_0^2}}\right] \quad (10)$$

The first distribution contains the crystallite size and stocking fault probability while the second one contains the microstrain of the lattice. Based on Fourier transform proprieties, the true sample function can be described by an equivalent relation,

$$f(s) = \int_{-\infty}^{\infty} P_C(s - s^*) P_G(s)\, ds \tag{11}$$

In the literature, relation (11) for explicit forms of P_C and P_G is called Voigt distribution. Unfortunately, the integral from eq. (11) can be performed only by numerical methods [24]. Because of this reason, many authors have considered that XRLP can be approximated by Voigt or pseudo Voigt (pV) distributions [25, 26]. The integral widths δ_C, δ_G of P_C and P_G distributions, expressed in the reciprocal space units are given by following relations,

$$\delta_C = \frac{1}{2D_{eff}}, \qquad \delta_G^2 = \frac{2\pi \left\langle \varepsilon_{hkl}^2 \right\rangle h_0^2}{a^2} \tag{12}$$

In terminology of P_C and P_G distributions, Fourier transform of the true sample, *F(L)*, is given by an equivalent relation,

$$\mathrm{F(L)} = \mathrm{e}^{-2\,\delta_C |L| - \pi\,\delta_G^2\, L^2}, \tag{13}$$

and its integral width can be expressed with another equivalent relation,

$$\delta^F(\delta_C, \delta_G) = \frac{1}{\delta_G} \exp\left(\frac{\delta_C^2}{\pi \delta_G^2}\right)\left[1 - \mathrm{erf}\left(\frac{\delta_C}{\sqrt{\pi}\delta_G}\right)\right] \tag{14}$$

The values of δ_C and δ_G for each observed XRLP can be refined by means of condition

$$\sum_L w_L \left[F_{hkl}^{calc}(L) - F_{hkl}^{\exp}(L)\right]^2 = \min, \tag{15}$$

where $F_{hkl}^{calc}(L)$, $F_{hkl}^{\exp}(L)$, w_L are given by eq. (13), Fourier transform of true sample obtained from experimental data, and weight factor.

3. Results and discussion

The analytical models were applied on two catalyst samples prepared by coprecipitation and impregnation. The following samples were investigated: 85 at. % Ni/Cr_2O_3 and 98.8 at. Ni/UO_2. The standard sample is a well annealed nickel black powder.

The X-ray diffraction (XRD) measurements were carried out at Beijing Synchrotron Radiation facilities (BSRF) in 4W1C beam lines operating at 30-50 mA and 2.2 GeV with an energy resolution of 1-3 eV at 10 KeV, at room temperature [27]. The X-ray wavelength for XRD experiments was adjusted to 1.8276 Å. A NaI (Ti) detector was used and the signals were amplified and fed to a single channel analyzer (ORTEC 850) read out by a computer.

Practically, it is not easy to obtain accurate values of the crystallite size and microstrain without extreme care in the experimental measurements and analysis of XRD data. The XRLP Fourier analysis validity depends strongly on the magnitude and nature of the error propagated in the data analysis. Three systematic errors have been discussed [23, 28]: uncorrected constant background, truncation and the effect of sampling the observed profile at a finite number of points that appear in the discrete Fourier analysis.

In order to minimize the propagation of these systematic errors a global approximation of the XRLP is adopted instead of the discrete Fourier analysis. Therefore, herein, the analysis of diffraction line broadening in X-ray powder pattern was analytically calculated using generalized Fermi function (GFF) facilities [16-20, 23].

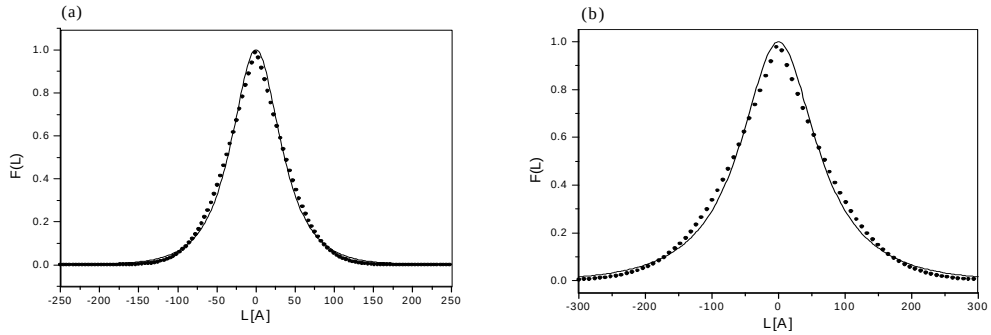

Fig. 2. Fourier transform of true samples (111) for Ni/Cr_2O_3 (a) and Ni/UO_2 (b); dots eq.(13), solid line ref. [16, 18].

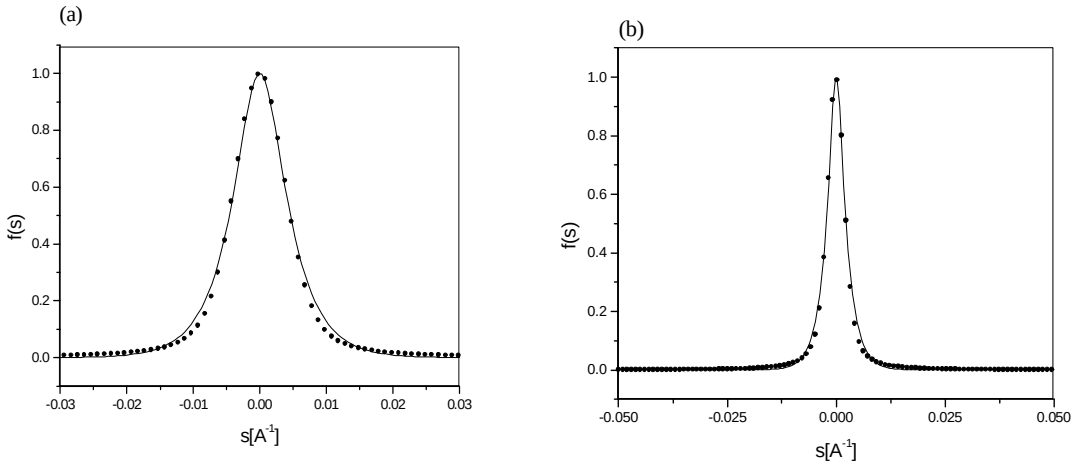

Fig. 3. The true sample function (111) for Ni/Cr_2O_3 (a) and Ni/UO_2 (b); dots analytical Voigt eq.(8), solid line ref. [16,18].

In this paper we analyze only (111) profiles. Their relative intensity for the investigated samples as well as for the standard sample with respect to the diffraction angle, after background correction, were presented [16]. Figs. 2(a) and 2(b) show the calculated Fourier transform of 85 at. % Ni/Cr_2O_3 and 98.8 at. Ni/UO_2 samples approximated by its analytical relation [16, 18] using GFF distributions for the experimental and instrumental functions and fitted by relation (3). Figs. 3(a) and 3(b) describe the true sample functions for the same catalysts obtained by the deconvolution technique and relation (8). In both cases the curves exhibit good similarities.

Table 2. Structural parameters of nickel supported catalysts investigated.

Name of sample	Integral widths				D_{eff} and $<\varepsilon^2>_{111}\times10^{-4}$			
	$\delta^{[g]}$ or $\delta^{[h]}$ $\times10^{-2}$ [1/Å] ref.[16,18]	$\delta^{[f]}$ $\times10^{-2}$ [1/Å] ref.[16,18]	$\delta^{[f]}_C$ and $\delta^{[f]}_G$ $\times10^{-2}$ [1/Å] rel. (12)	$\delta^{[F]}$ [Å] rel.(5,14)	pol. approx. ref.[12-20]		rel. (3)	Scherrer ref. [14]
					2^{nd} ord [Å]	3^{rd} ord [Å]	[Å]	[Å]
Ni black	0.2852	-	-	-	-	-	-	-
Ni/ Cr_2O_3	1.2070	1.1230	0.5682 0.7568	86	69 0.3636	62 0.4065	88 0.3773	178 -
Ni/ UO_2	0.7209	0.5852	0.3731 0.3343	165	148 0.1235	164 0.1308	134 0.0736	342 -

The main results regarding the investigated supported nickel catalysts are summarized in Table 2. The second up to fourth columns contain the integral widths of the instrumental and experimental profiles, the true sample and its Cauchy and gaussian contributions of XRLP expressed in reciprocal space units. The fifth column gives the integral width of the Fourier transform. The integral widths of the true sample functions and its Fourier transform are in agreement with relation (7). The next three columns contain the crystallite size and microstrain parameters determined by the 2^{nd} and 3^{rd} polynomial approximation [12-20] and relation (13) of the *F(L)* distribution, respectively. The last one indicates the crystallite size of investigated samples calculated by Scherrer formula.

There are large differences between global structural parameters corresponding to each computation technique. The nanostructural parameters determined by polynomial appro-ximations are very sensitive to the interval limits chosen for the fitting technique. The literature does not indicate a reliable prescription for choosing them. This situation is caused by the fact that the *F(L)* function is approximated only by a polynomial portion. In spite of many published results, we consider that polynomial approximations give reliable information for structural parameters only for large value of the integral width, that means crystallite size less than about 150 Å.

The most valuable formula for global microstructural information obtainable from XRLP analysis is general relation (13). This relation is valid for any value of *L* variables and it is not sensitive for interval chosen because the Fourier transform of the true sample is defined on the whole real axis. Our results determined by polynomial distributions are based on approximations when $L\rightarrow0$ from the relation (13). The definition interval is moved until the obtained results are similar to the ones obtained with the general formula.

In many cases, in literature are reported results obtained only by Scherrer relation, for quite large values of the integral width, without taking into account the contribution of the disorder parameter to the line shape. This can be reflected in ambiguous results.

The microstrains of lattice can also be correlated with the effective crystallite size in the following ways: the value of the effective crystallite size increases when the microstrain value decreases, and reverse.

5. Conclusions

In the present paper it is presented a theoretical analysis of X-ray line profile applied to the global structure determination of the supported nickel catalysts used in reactions as: reduction, oxidation, hydrogenation and isotopic exchange between hydrogen and deuterium. Their global structures can be correlation with the intrinsic catalytic activity. The conclusions that can be drawn from this study are:

(i) For XRLP analysis, a global approximation by GFF distribution is applied rather than a numerical Fourier analysis. This can minimize the systematic errors that appear in the traditional Fourier analysis;

(ii) The approximate forms of the Fourier transform are valid only for small crystallite size, less than 150 Å, and its general form can also be used use for any value of the variable *L*;

(iii) The new analytical true sample function and its approximation is one of the most general formula that contains the Cauchy and gaussian contributions;

(iv) XRSIZE package program contains all the methods described in the second section and it has a user's friendly interface.

References

[1] B. E. Warren, X-Ray Diffraction, Addison-Wesley Publishing Company, 1969.
[2] E. O. Brigham, The Fast Fourier Transform, Pretice-Hall Inc., Englewood Clifs, New Jersy, 1974.
[3] Tihonov and V. Arsenine, Méthodes de Résolution des Problèmes Mal Posés, Ed. Mir, Moscou, 1974.
[4] H. J. J. Te Riele, A program for solving first Fredholm integral equations by means of regularization, Report NM-R8416 of Center for Mathematics and Computer Sciences, 1984.
[5] Beniaminy, M. Deutsch, Comput. Physics Common. **21**, 271 (1980).
[6] H. P. Klug, L. E. Alexander, X-Ray Diffraction Procedures for Polycrystalline and Amorphous Materials, 2nd ed. John Wiley and Sons, New York 1974.
[7] F. Raiteri, A. Senin, G. Fagherazzi, J. Mater. Science **13**, 1717 (1978).
[8] R. S. Smith, IBM J. Res. Develop. **4**, 205 (1960).
[9] G. B. Mitra, N. K. Misra, Acta Cryst. **22**, 454 (1967).
[10] J. Mignot, D. Rondot, Acta Met. **23**, 1321 (1975).
[11] J. Mignot, D. Rondot, Acta Cryst. **33**, 327 1977.
[12] E. J. Charlson, D. H. Hu, M. R. Farukhi, Adv. X-Ray Anal. **14**, 441 (1871).
[13] P. Ganesen H. K Kuo, A. Saavedra, J. Catal. **52**, 310 (1978).
[14] N. Aldea, E. Indrea, Comput. Phys. Commun **60**, 155 (1990).
[15] N. Aldea, R. Zapotinschi, C. Cosma, Fresenius J. Anal. Chem. **355**, 367 (1995).
[16] N. Aldea, A. Gluhoi, P. Marginean, C. Cosma, X. Yaning, Spectrochim. Acta Part B **55**, 997 (2000).
[17] N. Aldea, A. Gluhoi, P. Marginean, C. Cosma, Xie Yaning,, H. Tiandou, W. Wu, B. Dong, Spectrochim. Acta Part B **57**, 1453 (2002).
[18] N. Aldea, C. V. Tiusan, B. Barz, J. Optoelectron. Adv. Mater. **6**(1), 225 (2004).
[19] N. Aldea, C. Tiusan, R. Zapotinschi, Proceedings of the 8th Joint EPS-APS International Conference on Physics Computing, Published by Academic Computer CYFRONET-Krakow, 1996, p. 391.
[20] N. Aldea, B. Barz, A. C. Gluhoi, P. Marginean X. Yaning H. Tiandou L. Tao, Z. Wu, Z. Wu, J. Optoelectron. Adv. Mater. **6**(4), 1287 (2004).
[21] P. Abramovich, I. A. Stegun, Handbook of Mathematical Function, Dower, New York 1965.
[22] J. S. Walker, Fast Fourier Transform, Second Ed. CRC Boca Raton , New Yrk London, Tokyo, 1997.
[23] N. Aldea, F. Aldea, Analysis Techniques of Physical-Chemical Signals, Ed. Risoprint, Cluj-Napoca, 2001 (in Romanian language).
[24] J. F. Kielkopf, J. Opt. Soc. Am. **63**(8) 987 (1973).
[25] Balzar, H. Ledbetter J. App. Cryst. **26**, 97 (1993).
[26] J. Mittemeijer, P. Scardi, Diffraction Analysis of the Microstructure of materials, Springer Verlag, Berlin, Heidelberg 2004.
[27] B. S. R. F. Activity Report 1991-2003, Beijing Electron Positron Collider, Coordination Laboratory of National Center for Nanoscience and Nanotechnology.
[28] R. A. Young, R. J. Gerdes, A. J. C. Wilson, Acta Cryst. **22,** 155 (1967).